

Tabulated values of water vapor pressure were used rather than the mass-spectrometer values, since these latter are not held to be reliable. The temperature of the cloud chamber was known immediately before expansion, so that the vapor pressure could be obtained from tables. This value of water vapor pressure was then

corrected to account for the known expansion ratio of the cloud chamber.

All that remained to be done at this point was to convert the proton ranges to alpha-particle ranges. The rule for this conversion is well-known for air and may be considered to be the same for oxygen.

Analysis of Some Deuteron-Induced Reactions in Oxygen-18†

J. C. ARMSTRONG* AND K. S. QUISENBERRY

Radiation Laboratory, University of Pittsburgh, Pittsburgh, Pennsylvania

(Received November 21, 1960)

The reactions $O^{18}(d,t)O^{17}$, $O^{18}(d,d')O^{18*}$, and $O^{18}(d,p)O^{19}$ are studied using 15-Mev deuterons and magnetic analysis of reaction particles. Absolute cross sections are determined for all reactions studied and the Butler-Born approximation is used to extract reduced widths when possible. Angular distributions of triton groups corresponding to the ground, 0.871-, 3.846-, 4.555-, 5.083-, and 5.378-Mev states of O^{17} are obtained. An estimate of the configuration admixtures in the O^{18} ground state is made from analysis of the reduced widths and indicates the presence of a sizable (about 6%) $(1f_{7/2})_0$ component. The experimentally determined admixtures are compared with several theoretical estimates. All O^{18} levels observed in the inelastic deuteron scattering have been previously reported—the known 5.01-Mev state is not observed. The angular distribution of inelastic deuterons corresponding to the 1.982-Mev state of O^{18} is obtained and comparison of the absolute cross section with theory provides an

estimate of the O^{18} deformation. Proton groups from $O^{18}(d,p)O^{19}$ reactions are observed corresponding to O^{19} excitations of 0, 1.469, 3.164, 3.948, (4.123), (4.586), (4.706), (5.165), 5.45, 5.707, and 6.279 Mev, where assignment of the levels in parentheses to O^{19} is uncertain. The known 0.096-Mev state is not observed and the proton group corresponding to 5.45-Mev excitation contains contributions from at least two states. Angular distributions leading to the O^{19} ground, 1.469-, 3.164-, 3.948-, 5.707-, and 6.279-Mev states are obtained and reduced widths extracted. The l_n values for these angular distributions are ambiguous except for the ground-state reaction ($l_n=2$) and the 1.469-Mev state reaction ($l_n=0$). Analysis of the data suggests that J^π (ground state) = $\frac{5}{2}^+$ and J^π (0.096-Mev state) = $\frac{3}{2}^+$. Using parameter values estimated from the O^{19} energy level spectrum or obtained from neighboring nuclei, a description of this nucleus in terms of the strong-coupling unified model agrees with the data.

I. INTRODUCTION

IN recent years nuclei just beyond O^{16} , at the beginning of the $1d-2s$ shell, have become increasingly important in the study of nuclear structure. They lie in a rather ill-defined region between nuclei described by shell model calculations ($A \leq 17$) and others described by the Bohr-Mottelson strong-coupling unified model¹ ($A \approx 25$). A theoretical description of the nuclei at the beginning of the $1d-2s$ shell may be possible solely in terms of one or the other of these two models, but will probably be complicated by interplay between independent-particle and collective effects.

Intermediate coupling calculations have been carried out for nuclei of $A = 18$ and 19 and satisfactorily explain the static properties of F^{18} , F^{19} , O^{18} , and O^{19} .²⁻⁴ Such calculations provide strong evidence for the validity

of an individual-particle, intermediate-coupling approach to these nuclei even though weak surface-particle coupling must be added to account for observed $E2$ transition rates.^{4,5} It is therefore surprising that F^{19} is also well described by the unified model in the strong-coupling limit.^{6,7} Such a description implies the importance of collective effects in F^{19} and possibly in neighboring nuclei as well, and suggests that there exists a fundamental equivalence between the individual-particle and collective-model theories.⁸

A study of deuteron-induced reactions in O^{18} will provide information about several light $1d-2s$ nuclei and may serve to clarify certain theoretical aspects of their structure. Analysis of the (d,t) reaction data should provide information about O^{17} but, more important, it may be used to deduce configuration admixtures in the O^{18} ground state. Inelastic deuteron scattering data are somewhat less informative, although recent theoretical studies indicate that nuclear deformations may possibly be obtained from inelastic scattering angular distri-

† Work done in the Sarah Mellon Scaife Radiation Laboratory and assisted by the joint program of the Office of Naval Research and the U. S. Atomic Energy Commission.

* Now at Physics Department, University of Maryland, College Park, Maryland.

¹ A. Bohr and B. R. Mottelson, *Kgl. Danske Videnskab. Selskab, Mat.-fys. Medd.* **27**, No. 16 (1955).

² M. G. Redlich, *Phys. Rev.* **95**, 448 (1954).

³ M. G. Redlich, *Phys. Rev.* **99**, 1427 (1955).

⁴ J. P. Elliott and B. H. Flowers, *Proc. Roy. Soc. (London)* **229**, 536 (1955).

⁵ F. C. Barker, *Phil. Mag.* **1**, 329 (1956).

⁶ E. B. Paul, *Phil. Mag.* **2**, 311 (1957).

⁷ G. Rakavy, *Nuclear Phys.* **4**, 375 (1957).

⁸ See for example: M. G. Redlich, *Phys. Rev.* **110**, 468 (1958); J. P. Elliott, *Proc. Roy. Soc. (London)* **A245**, 128 (1958); **A245**, 562 (1958).

butions.^{9,10} An investigation of the O¹⁸(*d,p*)O¹⁹ reactions will yield the energy level spectrum of O¹⁹ and the measured reduced widths should provide valuable information concerning the internal structure of this nucleus.

II. EXPERIMENTAL PROCEDURE

The experiments described below were performed utilizing 15-Mev deuterons from the University of Pittsburgh cyclotron. The magnetically analyzed beam on the target has an energy spread of only 40 keV but analysis of known reaction particle energies indicates that the mean incident energy is not constant. Daily energy variations of as much as 100 keV are not infrequent and the incident energy during these experiments ranged from 14.8 to 15.3 MeV.

The beam intensity transversing the target (0.1 to 1.0 μ A) is continuously monitored by collection in a Faraday cup. Through electronic integration of the Faraday cup current, reaction particle yields are measured for a predetermined incident charge. Normally the error associated with this integration is less than 1% and hence negligible, but for scattering angles between 5° and 9° it is necessary to use a smaller Faraday cup and the error is about $\pm 5\%$.

Reaction products are momentum analyzed by a 60°-sector magnet and detected either by CsI(Tl) crystal scintillators or by nuclear emulsion plates. The energy resolution of the system is typically 50 to 100 keV. Particle identification is accomplished by pulse-height analysis, using standard multichannel techniques, or by emulsion track grain density observation. Aluminum absorbers of appropriate thickness are used as needed to facilitate identification and detection of desired reaction particles in the presence of background.

The targets used in these experiments were oxidized nickel prepared by radiantly heating 5×10^{-5} -in. thick nickel foils in the presence of pure oxygen gas.¹¹ Targets having an oxygen areal density of 0.17 mg/cm² were prepared using natural O¹⁶, 38% enriched O¹⁸, and 98.2% enriched O¹⁸.¹² The total areal density of each target was 0.73 mg/cm² and represented an energy loss of 55 keV for the incident 15-Mev deuterons. It was found that these targets were highly stable against oxygen loss, the measured yields of reaction products remaining constant even after long exposure to the incident beam.

The 38% enriched O¹⁸ targets were used to determine all absolute cross sections through comparison with the O¹⁶(*d,p*)O¹⁷ ground-state reaction. The latter cross

section has been measured at this laboratory to be 34.0 ± 8.5 mb/sr at the peak of its angular distribution ($\theta_{c.m.} \approx 13^\circ$).¹³ Apart from other uncertainties introduced in the O¹⁸ experiments, the error in this value introduces an uncertainty of $\pm 25\%$ in all absolute cross sections reported here. The only other significant experimental errors are the statistical errors of accumulated counts, beam integration error, and the error introduced by the presence of a background produced by reactions in nickel. This background prevented accurate energy and cross section measurements of the low intensity peaks and represents the major disadvantage in using nickel oxide targets for this investigation. The total error in relative cross-section measurements varies from about 5% for the high-cross-section reactions to as much as 50% for those with low cross section.

III. DATA ANALYSIS AND DISCUSSION

The analysis of deuteron stripping and pickup reactions presented here makes use of reduced widths obtained by comparing experimental angular distributions with curves calculated using the Butler-Born approximation.¹⁴ It is well known that reduced widths extracted by this procedure are far smaller than those obtained from reasonable theoretical considerations and that these experimentally determined reduced widths may not be directly compared with theoretical results.¹⁵ Instead, the values of the single-particle reduced widths are considered empirical quantities to be determined experimentally.

The use of the Butler-Born approximation to extract reduced widths has been thoroughly discussed by Macfarlane and French.¹⁶ The approximation is viewed as a theory of three parameters: l_n , the orbital angular momentum of the transferred nucleon; r_0 , the stripping radius; and Θ^2 , the reduced width.¹⁷ Further $\Theta^2 = \mathcal{S}\Theta_0^2$ where \mathcal{S} , the spectroscopic factor, is proportional to the square of the overlap integral between initial and final states. The single-particle reduced width, Θ_0^2 , is equal to $\frac{1}{3}r_0^3 R_l^2(r_0)$, where $R_l(r)$ is the radial wave function of the transferred nucleon.

The values of r_0 and l_n are chosen so that the theoretical curve best fits the experimental data. The value of Θ^2 is then obtained through normalization of the theoretical expression to the observed absolute cross section. To determine \mathcal{S} it is assumed that the value of the relevant single-particle reduced width may be

¹³ E. W. Hamburger, Ph.D. thesis, University of Pittsburgh, 1959 (unpublished).

¹⁴ S. T. Butler and O. H. Hittmair, *Nuclear Stripping Reactions* (John Wiley & Sons, Inc., New York, 1957).

¹⁵ J. B. French, *Nuclear Spectroscopy*, edited by F. Ajzenberg-Selove (Academic Press, Inc., New York, 1960).

¹⁶ M. H. Macfarlane and J. B. French, *Revs. Modern Phys.* **32**, 567 (1960).

¹⁷ All reduced widths reported here are extracted by the methods outlined in reference 14 and include the isotopic spin coupling factor assuming $T = \frac{1}{2}$, 1, and $\frac{3}{2}$ for all relevant states in O¹⁷, O¹⁸, and O¹⁹, respectively.

⁹ J. S. Blair, *Phys. Rev.* **115**, 928 (1959).

¹⁰ E. Rost and N. Austern (to be published).

¹¹ H. D. Holmgren, J. M. Blair, K. F. Famularo, T. F. Stratton, and R. V. Stuart, *Rev. Sci. Instr.* **25**, 1026 (1954).

¹² The 38% enriched O¹⁸ containing 56.2% O¹⁶, 0.85% O¹⁷, and 37.9% O¹⁸ was furnished through the courtesy of A. O. Nier, University of Minnesota. The concentrated O¹⁸ containing 0.9% O¹⁶, 0.985% O¹⁷, and 98.2% O¹⁸ was purchased from the Weizmann Institute of Science, Rehovoth, Israel.

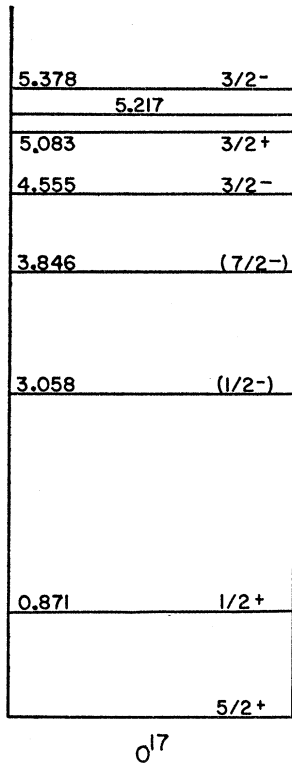


FIG. 1. Energy level diagram of O¹⁷. Energy values (Mev) and J^π assignments are taken from Ajzenberg-Selove and Lauritsen, reference 20.

taken from analyses of experiments in neighboring nuclei.

The analysis presented here cannot yield exact results because uncertainties in both experimental data and the treatment of reduced widths introduce unavoidable errors. The reliability of quantitative conclusions can only be judged by their internal consistency. The uncertainty in all reduced widths used here is taken to be approximately 25%.

A. O¹⁸(d,t)O¹⁷ Reactions

Pickup reactions in light and medium-weight nuclei connecting states of known spin and parity offer a direct method for determination of the target nucleus ground-state (g.s.) wave function. Uncertainties in single-particle reduced width values and necessary approximations in reaction data analysis limit the accuracy of the results. Nonetheless such reactions have yielded valuable information in determining the approximate strengths of configuration admixtures in some nuclei.^{18,19} The reaction O¹⁸(d,t)O¹⁷ is well suited for such a wave function determination. The Q value of the ground-state reaction is -1.81 Mev, which results in relatively high triton energies and makes detection considerably less difficult than is usually the case. Further, the residual nucleus in this reaction has been

¹⁸ E. Baranger and S. Meshkov, Phys. Rev. Letters **1**, 30 (1958).

¹⁹ E. W. Hamburger and A. G. Blair, Phys. Rev. **119**, 777 (1960).

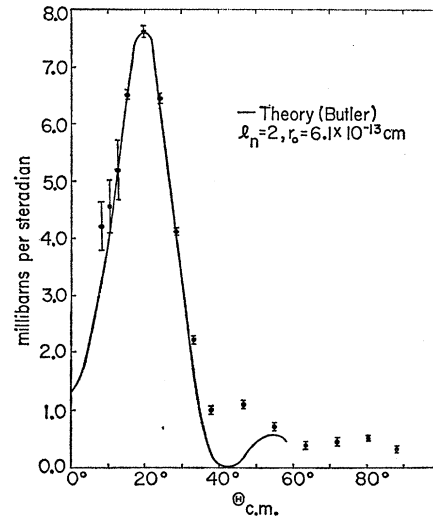


FIG. 2. Angular distribution of the O¹⁸(d,t)O¹⁷ ground state.

well studied and seven of the first eight levels in O¹⁷ have either certain or probable spin and parity assignments as shown in Fig. 1.²⁰ The spin and parity of the O¹⁸ g.s. is known to be 0⁺.

1. Experimental Data

Triton groups corresponding to the ground state and first seven excited states of O¹⁷ have been observed and six angular distributions obtained. Triton identification was accomplished by pulse-height analysis and level assignments for the various triton groups were made by energy analysis.

Absolute cross sections measured at three laboratory angles are listed in Table I. The 5.22-Mev state was

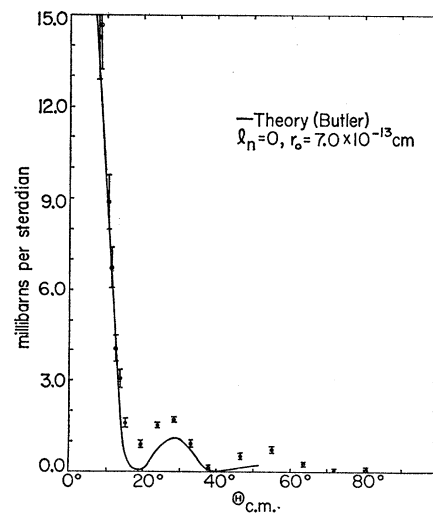
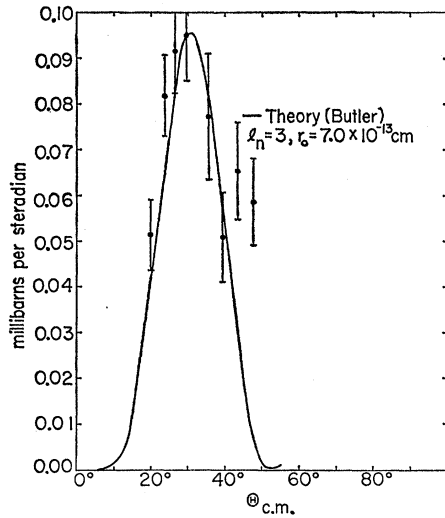
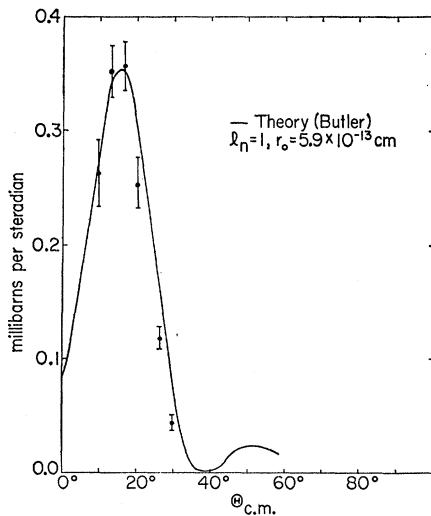
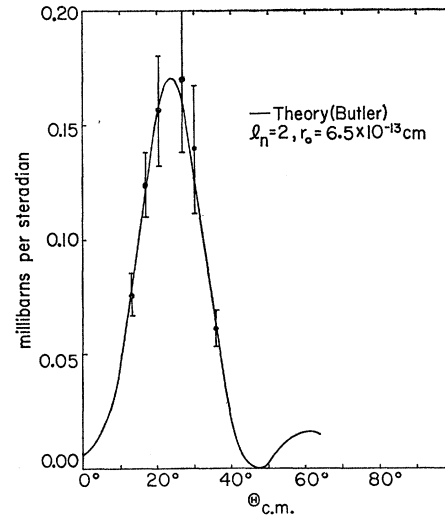


FIG. 3. Angular distribution of the O¹⁸(d,t)O¹⁷ 0.871-Mev state.

²⁰ Unless otherwise specified, Q values, excitation energies, spin, and parity assignments quoted herein have been taken from F. Ajzenberg-Selove and T. Lauritsen, Nuclear Phys. **11**, 1 (1959).


 FIG. 4. Angular distribution of the $O^{18}(d,t)O^{17}$ 3.846-Mev state.

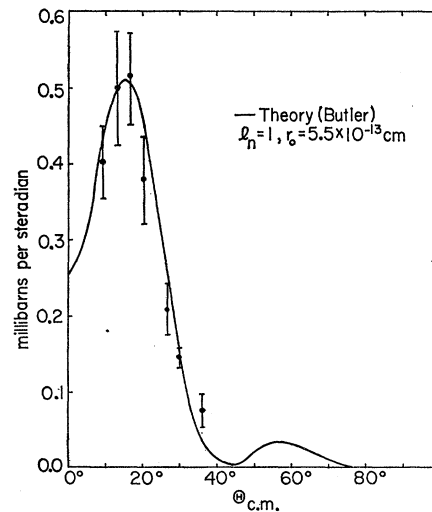
only weakly excited, the maximum observed cross section being <0.07 mb/sr at $\theta_{lab}=14^\circ$, so that no angular distribution of this group was obtained. The cross section for excitation of the 3.058-Mev state was large at both $\theta_{lab}=8^\circ$ and $\theta_{lab}=35^\circ$, but detection between these angles was prevented by the presence of the very intense elastic deuteron group. Angular distributions of triton groups corresponding to the ground, 0.871-, 3.846-, 4.555-, 5.083-, and 5.378-Mev states together with curves calculated using the Butler-Born approximation are shown in Figs. 2 through 7. The stripping radius r_0 has been adjusted to give the best fit for each set of data and is shown in each figure. All l_n values used are in accord with the spin and parity assignments of Fig. 1. The only uncertain l_n assignment is that for the 3.846-Mev ($7/2^-$) state. Theoretical curves for this reaction having $l_n=1, 2,$ and 3 require


 FIG. 5. Angular distribution of the $O^{18}(d,t)O^{17}$ 4.555-Mev state.

 FIG. 6. Angular distribution of the $O^{18}(d,t)O^{17}$ 5.083-Mev state.

stripping radii of 2.0, 4.7, and 7.0 fermis, respectively. Because the r_0 values for all other levels observed are between 5.5 and 7.0 fermis the $l_n=3$ curve and consequently a $5/2^-$ or $7/2^-$ spin and parity assignment is favored.

2. O^{18} Ground-State Wave Function and Reduced Width Values

The direct extraction of nuclear spectroscopic information from a (d,t) reaction is currently impossible because the deuteron-triton stripping transform is not numerically calculable. As a recourse, one obtains from the data not Θ^2 , but $\Lambda\Theta^2$ where Λ arises from the uncertainty in the value of the deuteron-triton stripping transform.²¹ The values of $\Lambda\Theta^2$ extracted from the data of Figs. 2 through 7 are listed in Table II.


 FIG. 7. Angular distribution of the $O^{18}(d,t)O^{17}$ 5.378-Mev state.

²¹ The quantity Λ is explicitly defined in reference (16).

If it is assumed that Λ is not a function of l_n and Q ,²² one may write

$$\Lambda\Theta^2/\Lambda\Theta'^2 = s\Theta_0^2/s'\Theta_0'^2, \quad (1)$$

and multiplication by $\Theta_0'^2/\Theta_0^2$ determines the ratio s/s' .

In order to extract from the data an estimate of the configuration mixture in the O^{18} g.s. wave function, two further assumptions are necessary. It is assumed that the observed positive parity states of O^{17} and the $(7/2^-)$ 3.846-Mev state are good single-particle states. That is, the wave function of each of these states is taken to be of the form

$$\Psi(O^{17})_J = \Psi(O^{16} \text{ g.s.})_{J=0} \times |nl_j\rangle_{j=J}, \quad (2)$$

where n , l , and j are the principal, orbital angular momentum, and total angular momentum quantum numbers, respectively, of the single neutron outside the O^{16} core. The O^{18} g.s. wave function is assumed to have the form

$$\Psi(O^{18} \text{ g.s.})_{J=0} = \Psi(O^{16} \text{ g.s.})_{J=0} \times \sum_j a_j |nl_j^2\rangle_0. \quad (3)$$

The spectroscopic factor for the (d,t) reaction connecting Eq. (2) with Eq. (3) is simply

$$S(j) = 2a_j^2, \quad (4)$$

and Eq. (1) may now be written

$$s\Theta_0^2/s'\Theta_0'^2 = a_j^2\Theta_0^2/a_j'^2\Theta_0'^2. \quad (5)$$

Hence the ratios of single-particle reduced widths, together with the normalization condition $\sum_j a_j^2 = 1$, determine the a_j^2 values uniquely. If the O^{18} g.s. wave function [Eq. (3)] contains only the extra core nl_j values $1d_{5/2}$, $2s_{1/2}$, $1d_{3/2}$, and $1f_{7/2}$, the single-particle reduced width ratios necessary to determine the a_j^2

TABLE I. $O^{18}(d,t)O^{17}$ measured absolute differential cross sections.

O^{17} energy level (Mev)	$\theta_{\text{lab}} = 11^\circ$ (except as noted) $d\sigma/d\Omega^a$ (mb/sr)	$\theta_{\text{lab}} = 25^\circ$ (except as noted) $d\sigma/d\Omega^a$ (mb/sr)	Maximum observed cross section $d\sigma/d\Omega^a$ (mb/sr)	θ_{lab}
g. s.	5.21 ± 0.57	4.12 ± 0.19	7.72 ± 0.08	17°
0.871	4.06 ± 0.30	1.71 ± 0.04	14.7 ± 1.5	7°
3.058	2.7 ^b ± 1.5	0.50 ^c ± 0.12	2.7 ^d ± 1.5	11°
3.846	0.051 ^e ± 0.007	0.095 ± 0.009	0.095 ± 0.009	25°
4.555	0.35 ± 0.02	0.044 ± 0.005	0.35 ± 0.02	15°
5.083	0.076 ± 0.011	0.14 ± 0.03	0.17 ± 0.04	17°
5.215	<0.03	<0.03	<0.07	14°
5.378	0.50 ± 0.07	0.29 ± 0.03	0.51 ± 0.07	11°

^a Errors quoted in this table are relative, absolute cross sections having been determined by assuming the $O^{18}(d,p)O^{17}$ g.s. reaction ($E_d = 15$ Mev) cross section is 34 mb/sr at the peak of its angular distribution ($\theta_{\text{c.m.}} \approx 13^\circ$). Reference (13). All absolute cross sections have an additional error of $\pm 25\%$.

^b $\theta_{\text{lab}} = 8^\circ$.
^c $\theta_{\text{lab}} = 37^\circ$.
^d The triton group corresponding to the 3.058-Mev level was not observed between $\theta_{\text{lab}} = 8^\circ$ and $\theta_{\text{lab}} = 37^\circ$.
^e $\theta_{\text{lab}} = 17^\circ$. This triton group was not studied at laboratory angles less than 17° .

²² The validity of this assumption is questionable. See reference (21) and A. I. Hamburger, Phys. Rev. **118**, 1271 (1960).

TABLE II. Parameters used in fitting theoretical curves to the $O^{18}(d,t)O^{17}$ angular distribution data.

Level	J^π	l_n	$r_0(f)$	$\Lambda\Theta^2$	$\Lambda\Theta^2/\Lambda\Theta_{\text{g.s.}}^2$
g.s.	5/2 ⁺	2	6.1	5.7	1
0.871	1/2 ⁺	0	7.0	2.2	0.74
3.846	(7/2 ⁻)	3	7.0	0.21	0.038
4.555	3/2 ⁻	1	5.9	0.22	0.039
5.083	3/2 ⁺	2	5.6	0.25	0.044
5.378	3/2 ⁻	1	5.5	0.39	0.066

are $\Theta_0^2(2s)/\Theta_0^2(1d)$ and $\Theta_0^2(1f)/\Theta_0^2(1d)$. These are assumed to have the values 2.0 and 0.5, respectively.²³ The resulting wave function (coefficients written as percentages) is

$$\Psi(O^{18} \text{ g.s.}) = \Psi(O^{16} \text{ g.s.}) \times \{76.4(1d_{5/2}^2)_0 + 14.7(2s_{1/2}^2)_0 + 3.3(1d_{3/2}^2)_0 + 5.6(1f_{7/2}^2)_0\}. \quad (6)$$

The correctness of this analysis depends upon the validity of Eqs. (1), (2), and (3). The numerical uncertainties in the coefficients of Eq. (6) result from both experimental inaccuracies and possible errors in the choice of Θ_0^2 ratios. The total error of each coefficient is estimated to be less than 20%.

The value of Λ , unnecessary in the above analysis, may be estimated from analyses of previous experiments at this laboratory. The experiments of Moore²⁴ and of Vogelsang and McGruer²⁵ have been analyzed and indicate $\Lambda = 165$ and 160, respectively.¹⁶ A reasonable value for use here is, therefore, $\Lambda = 160$. With this value of Λ and the a_j^2 values taken from Eq. (6) the single-particle reduced widths are

$$\Theta_0^2(1d) = 0.024; \quad \Theta_0^2(2s) = 0.05; \quad \Theta_0^2(1f) = 0.012.$$

These values agree well with those obtained from analyses of reactions involving comparable binding energies of the transferred nucleon.¹⁶ Finally, the (total) reduced widths for the $l_n = 1$ transitions, again using $\Lambda = 160$, are

$$\Theta^2(4.555\text{-Mev state}) = 0.0014, \\ \Theta^2(5.378\text{-Mev state}) = 0.0024.$$

3. Estimates of Configuration Mixing in O^{18}

a. Shell model. The necessity of strong $1d$ - $2s$ configuration mixing in describing the properties of the $A = 18$ and 19 isotopes of oxygen and fluorine is indicated by the intermediate-coupling calculations of Redlich^{2,3} and of Elliott and Flowers.⁴ Neither of the calculations

²³ The $2s$ and $1d$ single-particle reduced widths extracted from experiments through use of the Butler-Born approximation and compiled in reference (16) exhibit a strong dependence on the binding energy of the transferred nucleon. The binding energies here are 7.3 and 8.2 Mev. The ratios quoted correspond to binding energies in this range. M. H. Macfarlane (private communication).
²⁴ W. E. Moore, Ph.D. thesis, University of Pittsburgh, 1959 (unpublished).

²⁵ W. F. Vogelsang and J. N. McGruer, Phys. Rev. **109**, 1663 (1958).

includes mixing of $N=3$ ($1f$ and $2p$) configurations, although Redlich examined this possibility for $A=18$ and found that the strongest mixing between ($1d_{5/2}$) and ($1f_{7/2}$) occurs for $T=1, J=0$ states and ordinary (Wigner) exchange forces. The amplitude of the admixture is small and not included in his subsequent calculations. An intermediate coupling calculation including ($1f_{7/2}$)₀ and ($2p_{3/2}$)₀ admixtures in the O¹⁸ g.s. has been made by Macfarlane and French.¹⁶ None of these calculations reproduce the experimentally observed energy level spectrum. They are, however, based upon reasonable parameter values so that the predicted O¹⁸ g.s. wave functions, shown in Table III, are considered good approximations to the predictions that would result from a more accurate intermediate-coupling calculation.

Each calculation is in agreement with experiment at least to the extent that it correctly predicts the experimentally observed ratios of the ($1d_{5/2}$)₀, ($2s_{1/2}$)₀, and ($1d_{3/2}$)₀ admixtures and the calculation of Macfarlane and French indicates that this method may be capable of correctly accounting for $N=3$ ($1f, 2p$) admixtures. The experimental uncertainties do not permit a conclusive comparison of the individual calculations.

b. Strong-coupling unified model. Successful descriptions of F¹⁹ in terms of the Bohr-Mottleson strong-coupling unified model indicate that this model might find general applicability in the light $1d$ - $2s$ shell.^{6,7} There has been presented some evidence to the contrary.²⁶ A comparison of the O¹⁸ g.s. configuration admixtures predicted by this model with those obtained experimentally would be useful as a further test for the model. The theoretical admixtures may be computed from the wave function tabulations of Nilsson.²⁷ These are dependent upon the nuclear deformation and in order to obtain the wave function listed in Table III it was assumed that the O¹⁸ deformation is approximately

TABLE III. Values found for the O¹⁸ ground-state configuration admixture coefficients a_j^2 , in percent.

	$1d_{5/2}$	$2s_{1/2}$	$1d_{3/2}$	$1f_{7/2}$	$2p_{3/2}$
Present experiment ^a	76.4	14.7	3.3	5.6	0
Present experiment ^{a, b}	81.0	15.5	3.5	0	0
Redlich ^c	74.0	16.4	9.6	0	0
Elliott and Flowers ^d	79.0	15.2	5.8	0	0
Macfarlane and French ^e	69.9	21.2	5.2	2.9	0.7
Nilsson ^f	74.6	20.0	5.4	0	0
Pairing force ^g	84.3	8.6	1.8	5.3	0

^a Admixture of ($2p_{3/2}$)₀ component is assumed to be negligible.

^b Renormalized experimental wave function neglecting ($1f_{7/2}$)₀ for comparison with theoretical wave functions.

^c Shell-model calculation, see reference 4.

^d Shell-model calculation, see reference 3.

^e Shell-model calculation, see reference 16.

^f Unified-model calculation assuming $\beta=0.2$, see reference 27.

^g $G=0.45$. See text.

²⁶ The low-lying (3.56-Mev) 4^+ state in O¹⁸ has been cited as rather conclusive evidence that this nucleus cannot be described by the strong-coupling unified model. H. E. Gove and A. E. Litherland, Phys. Rev. **113**, 1078 (1959).

²⁷ S. G. Nilsson, Kgl. Danske Videnskab. Selskab, Mat.-fys. Medd. **29**, No. 16 (1955).

two thirds the deformation used to describe F¹⁹. The admixture predictions are in reasonable agreement with experiment and suggest the possibility of describing successfully O¹⁸ by this model. Further data are necessary to confirm or reject this possibility.

c. Pairing force. Recently a probable candidate for the first excited 0^+ state in O¹⁸ has been found at 3.65 Mev.²⁸ Knowledge of its excitation energy allows one to make an elementary pairing force calculation to derive configuration mixtures in the $T=1, J=0$ states of O¹⁸, adjusting the pairing force strength G to reproduce the observed energy splitting of the ground state and this first excited 0^+ state. Single-particle energies ϵ_j are taken from O¹⁷ and the Hamiltonian is of the form²⁹

$$H = \sum_{jm} \epsilon_j b_{jm}^\dagger b_{jm} - \frac{G}{2} \sum_{ii'} \sum_{mm'} b_{j'm'}^\dagger b_{j'-m'}^\dagger b_{j-m} b_{jm}, \quad (7)$$

where b_{jm}^\dagger and b_{jm} are creation and annihilation operators, respectively, for a particle with total angular momentum j and magnetic quantum number m . The resulting energy matrix is

$$\begin{matrix} 1d_{5/2} \\ 2s_{1/2} \\ 1f_{7/2} \\ 1d_{3/2} \end{matrix} \begin{pmatrix} -3G & -\sqrt{3}G & -(12)^{1/2}G & -\sqrt{6}G \\ -\sqrt{3}G & 1.74-G & -2G & -\sqrt{2}G \\ -(12)^{1/2}G & -2G & 7.72-4G & -\sqrt{8}G \\ -\sqrt{6}G & -\sqrt{2}G & -\sqrt{8}G & 10.16-2G \end{pmatrix}.$$

A 3.6-Mev energy splitting between the ground state and first excited 0^+ state is produced with a value of $G=0.45$ Mev. The resulting g.s. wave function has the following components:

$$84.3\% (1d_{5/2}), 8.6\% (2s_{1/2}), 1.8\% (1d_{3/2}), \\ \text{and } 5.3\% (1f_{7/2}).$$

In agreement with experiment, the pairing force calculation predicts that the ($1f_{7/2}$) component is larger than the ($1d_{3/2}$). It does underestimate the ($2s_{1/2}$) admixture and the value of $G(\approx 8/A)$ is somewhat smaller than one might expect in this region of A .³⁰ The validity of this calculation is therefore considered to be questionable.

4. Odd-Parity Transitions

a. 3.846-Mev state. The analysis of the data presented above is based on the validity of several rather severe assumptions. The existence of single-particle $1d_{5/2}, 1d_{3/2}, 2s_{1/2}$, and $1f_{7/2}$ states in O¹⁷ is essential to the entire project. While there is no conclusive evidence to the contrary, such an assumption for the ($7/2^-$) 3.846-Mev state is perhaps premature. Recent data obtained by Keller indicate that the reduced width for the (d, p) reaction to this level from O¹⁶ is far less than the $1f$

²⁸ H. E. Gove (private communication).

²⁹ L. S. Kisslinger and R. A. Sorenson (to be published).

³⁰ In Mg²⁴, $G \approx 18/A$; see reference 19.

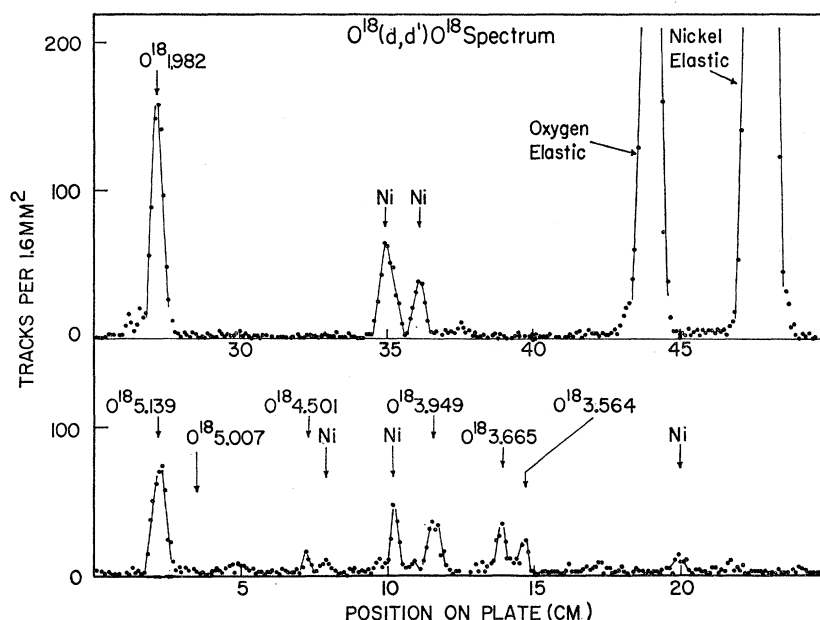


FIG. 8. Nuclear emulsion plate inelastic deuteron spectrum at $\theta_{\text{lab}}=35^\circ$. Arrows denote the expected position of known levels.

single-particle reduced widths obtained from reactions studied in neighboring nuclei.³¹

Another complication arises in analyzing the $l_n=3$ reaction data. Even if the 3.846-Mev state is a single $1f_{7/2}$ neutron state, it has been shown that such a state in O^{17} (where the $1d_{5/2}$ subshell is not filled) is approximately 15% spurious and thus must contain at least this percentage of core excited configurations.³² The $(1f_{7/2}^2)$ component in the O^{18} ground state is likewise impure, the wave function of such a configuration having the form

$$\Psi(1f_{7/2}^2) \approx (0.7)^{1/2}(1f_{7/2}^2) + (0.3)^{1/2}(\text{core excitation}). \quad (8)$$

Consequently the assumption of a calculable spectroscopic factor for this transition ($S=2a_{7/2}^2$) must be viewed as a crude approximation. A correct calculation of this spectroscopic factor requires knowledge of the degree of overlap between the core excited configurations in the $(1f_{7/2})_{7/2}$ and $(1f_{7/2})_0$ wave functions and knowledge of the relative phases of the various components. Assuming as limits perfect core overlap and no core overlap, the method used above to determine the O^{18} g.s. admixtures may overestimate the $(1f_{7/2}^2)_0$ component by 10% or underestimate it by a factor of two. The complete wave functions necessary for an exact calculation are not available, but it can be shown that the core overlap integral does not vanish.³³

b. 4.555- and 5.378-Mev States. The extraction of quantitative spectroscopic information from analysis of the $l_n=1$ transitions is also complicated by the fact that the wave functions of the relevant states are not known and hence the overlap integrals cannot be

calculated. Analysis of $O^{16}(d,p)O^{17}$ data yields a larger reduced width for the 4.555-Mev state than for that at 5.378-Mev, the sum being considerably less than the full $2p$ single-particle reduced width.³¹ This indicates that although the 4.555-Mev state possesses a larger $(O^{16} \times 2p_{3/2})_{3/2}$ component than the 5.378-Mev state, both states contain admixtures of at least two other configurations. The $O^{18}(d,t)O^{17}$ data suggest that one of these configurations is $(O^{18} \times 1p_{3/2}^{-1})_{3/2}$, but further (quantitative) conclusions are impossible.

c. 3.058-Mev State. No angular distribution of the triton group corresponding to the 3.058-Mev state in O^{17} was obtained. If the J^π of this state is $\frac{1}{2}^-$, its strong excitation in the $O^{18}(d,t)O^{17}$ reaction indicates a large overlap of the wave function and that of the configuration $(O^{18} \times 1p_{1/2}^{-1})_{1/2}$. The configuration previously proposed $[(C^{12} \text{ g.s.})_{J=0} \times (2s_{1/2}^2 1p_{1/2})_{1/2}]$ may be present in this state but it is unlikely that this configuration accounts for the large cross section.³⁴

B. $O^{18}(d,d')O^{18}$ * Reactions

Detailed interpretation of inelastic deuteron scattering in terms of nuclear spectroscopy is at present more difficult than analysis of deuteron stripping and pickup reactions. The information obtained from data presented here is therefore limited to energy values of some excited states and a questionable estimate of the deformation of the O^{18} nucleus.

Inelastically scattered deuterons corresponding to excitations in O^{18} up to 5.5 Mev were observed at laboratory scattering angles of 17° , 25° , and 35° . A typical spectrum ($\theta_{\text{lab}}=35^\circ$) is shown in Fig. 8 and partial spectra ($\theta_{\text{lab}}=17^\circ$ and 25°) appear in Fig. 9. Similar spectra obtained from a pure nickel target indicate that

³¹ E. L. Keller, Phys. Rev. **121**, 820 (1961).

³² E. Baranger and C. W. Lee, Nuclear Phys (to be published).

³³ E. Baranger (private communication).

³⁴ I. Unna and I. Talmi, Phys. Rev. **112**, 452 (1958).

TABLE IV. Experimentally determined Q values for the $O^{18}(d,d')O^{18*}$ reactions in Mev.

Level ^a	$\theta_{lab}=17^\circ$	$\theta_{lab}=25^\circ$	$\theta_{lab}=35^\circ$	av Q value ^d
1.982 ± 0.004^b	1.982	1.982	1.982	
3.550 ± 0.020	3.557	3.565	3.570	3.564 ± 0.025
3.639 ± 0.015^c	3.653	3.654	3.657	3.655 ± 0.030
3.929 ± 0.040	3.949	3.946	3.952	3.949 ± 0.030
4.457 ± 0.015^c	4.498	4.503	...	4.501 ± 0.040
5.007 ± 0.040	not observed			
5.170 ± 0.040	5.134	5.142	5.141	5.139 ± 0.030
5.311 ± 0.040	5.294	5.302	5.306	5.301 ± 0.030
5.456 ± 0.040	5.414	5.411	...	5.413 ± 0.035

^a Energies quoted by Ajzenberg-Selove and Lauritsen, reference 20, except as noted.

^b Q values measured relative to the 1.982-Mev state.

^c Energy assignments by N. Jarmie and M. G. Silbert, reference 35.

^d Errors quoted are estimated probable errors.

the major portion of the background originates from $Ni(d,d')Ni^*$ reactions.

The Q value of each $O^{18}(d,d')O^{18*}$ reaction was measured relative to that of the first excited state ($Q=1.982 \pm 0.004$ Mev). An error of ± 20 kev is introduced by the magnetic analyzer absolute calibration and additional error results in determining the relative laboratory energy of deuteron groups. The unweighted average of three Q -value measurements is given in Table IV together with its estimated probable uncertainty.

All of the O^{18} states observed in this experiment have been previously reported. The 3.655- and 4.501-Mev states are not listed by Ajzenberg-Selove and Lauritsen, but were observed recently in the reaction $O^{16}(t,p)O^{18}$

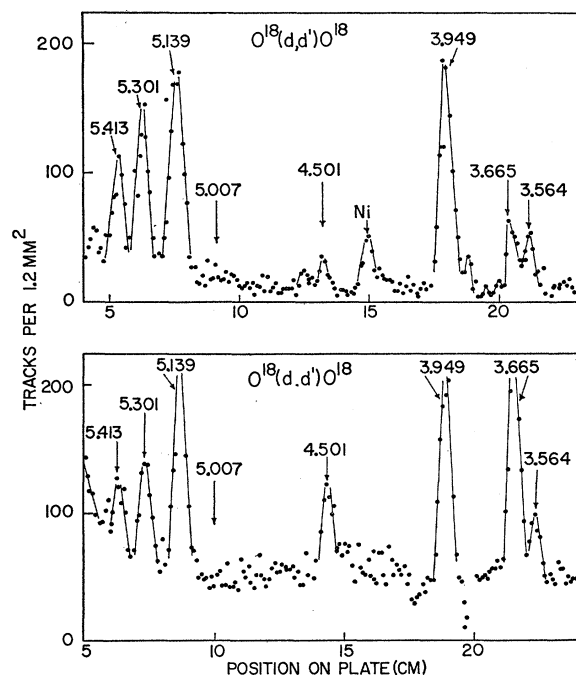


Fig. 9. Partial spectra of inelastic deuteron scattering obtained at $\theta_{lab}=25^\circ$ (top) and $\theta_{lab}=17^\circ$ (bottom). Arrows denote the position of energy levels in O^{18} .

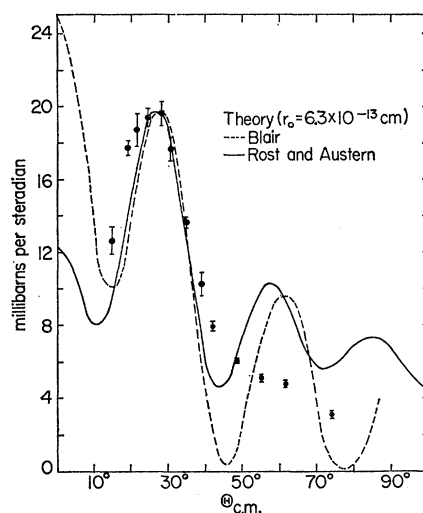


Fig. 10. Measured angular distribution of the $O^{18}(d,d')O^{18}$ 1.982-Mev state and the theoretical curves (reference 9 and 10) fitted to the data.

by Jarmie and Silbert who measured values of 3.639 ± 0.015 and 4.457 ± 0.015 Mev, respectively, in reasonable agreement with those obtained here.³⁵ The 5.007-Mev state was not observed. Absolute cross sections obtained from the data appear in Table V.

The large cross section for excitation of the 1.982-Mev first excited state prompted an investigation of the angular distribution of the corresponding deuteron group. The data are shown in Fig. 10 together with two theoretically predicted curves.^{9,10} These calculations have been shown to be similar,¹⁰ the former making use of plane waves and the adiabatic assumption while the latter is a distorted wave Born approximation. The degree of applicability of these theories to inelastic deuteron scattering is uncertain. Approximately correct values of the nuclear deformation parameter β have

TABLE V. $O^{18}(d,d')O^{18*}$ measured absolute differential cross sections.

O^{18} energy level (Mev)	$\theta_{lab}=17^\circ$ $d\sigma/d\Omega^a$ (mb/sr)	$\theta_{lab}=25^\circ$ $d\sigma/d\Omega^a$ (mb/sr)	$\theta_{lab}=35^\circ$ $d\sigma/d\Omega^a$ (mb/sr)
1.982	17.7 ± 0.4	19.7 ± 0.6	10.0 ± 0.3
3.564	1.03 ± 0.13	0.92 ± 0.08	1.10 ± 0.09
3.655	4.69 ± 0.19	1.09 ± 0.09	0.19 ± 0.11
3.949	4.27 ± 0.17	4.69 ± 0.19	2.17 ± 0.13
4.501	1.52 ± 0.14	0.42 ± 0.08	0.13 ± 0.09
5.01 ^b	< 0.14	< 0.10	< 0.034
5.139	3.99 ± 0.20	4.16 ± 0.17	4.44 ± 0.18
5.301	2.05 ± 0.14	3.08 ± 0.15	1.37 ± 0.12
5.413	1.30 ± 0.13	1.58 ± 0.13	

^a Errors quoted in this table are relative, absolute cross sections having been determined by assuming the $O^{16}(d,p)O^{17}$ g.s. reaction ($E_d=15$ Mev) cross section is 34 mb/sr at the peak of its angular distribution ($\theta_{c.m.} \approx 13^\circ$). See reference 13. All absolute cross sections quoted have an additional error of $\pm 25\%$.

^b 5.01-Mev level was not observed. Entries in cross-section columns for this level are statistical upper limits.

³⁵ N. Jarmie and M. G. Silbert, Phys. Rev. **120**, 914 (1960).

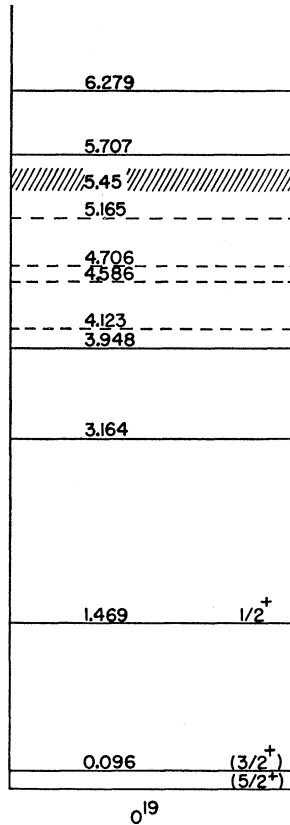


FIG. 11. Energy level diagram of O^{19} . Dashed lines represent levels whose assignment to O^{19} are uncertain. The broad level at 5.45 Mev is definitely associated with O^{19} and contains contributions from at least two separate states. The 0.096-Mev state was not observed in this experiment.

been obtained however by fitting Blair's theoretical curves to inelastic deuteron scattering data in the magnesium isotopes.³⁶ It is therefore of interest to compare the O^{18} deformation thus extracted with reasonable estimates. For interaction radii of 6.3 and 6.7 fermis, Blair curves yield β values of 0.26 and 0.23, respectively. Both of these values are somewhat larger than the value 0.20 assumed to obtain the O^{18} g.s. wave function listed in Table III and smaller than the theoretical prediction $\beta \approx 0.27$ of Rakavy.⁷

The theoretical curves fit the experimental data quite well in the region of the observed first maximum, but both predict a more pronounced oscillatory pattern than is observed experimentally. More experimental data are necessary in order to make a detailed comparison.

C. $O^{18}(d,p)O^{19}$ Reactions

1. Data

A search for proton groups corresponding to energy levels in O^{19} up to 9-Mev excitation was made at three laboratory scattering angles ($11^\circ, 17^\circ, 25^\circ$) and the results are shown in Table VI. The excitation energy values were obtained from Q values measured relative to the second excited state whose excitation energy is

1.469 ± 0.011 Mev. The energy errors quoted in Table VI are estimated probable uncertainties. Assignment of the proton groups to energy levels in O^{19} was verified wherever possible by accurate determination of the angular dependence of reaction proton energies. This dependence could not be determined with sufficient accuracy to differentiate between target nuclei of $A = 17, 18,$ and 19 . Further, the low cross-section peaks could not be observed over a sufficiently large angular interval to make this test. Data obtained using targets of different oxygen isotopic ratio indicate it to be unlikely that any levels assigned to O^{19} arise from other oxygen isotopes. All levels assigned to O^{19} are summarized in Table VI and presented in Fig. 11. Levels whose assignment to O^{19} is uncertain are parenthesized in Table VI and shown as dashed lines in Fig. 11.

The background originating from deuteron-induced reactions in nickel caused considerable difficulty. A proton spectrum ($\theta_{lab} = 17^\circ$) is shown in Fig. 12. While some groups corresponding to O^{19} levels are well above the background and offer the possibility of accurate Q value and cross-section determination, other smaller groups are interlaced with both nickel and O^{17} groups and do not. For this reason no attempt was made to obtain angular distributions of the proton groups corresponding to probable O^{19} states at 4.123, 4.586, and 4.706 Mev. The 0.096-Mev state was not observed and the cross sections for it listed in Table VI are statistical upper limits. Upper limits for the cross section of other unobserved O^{19} states (assuming that their full width at half maximum is less than 200 kev) are 0.8, 0.5, and 0.4 mb/sr below 5 Mev and 1.8, 1.3, and 0.97 mb/sr above 5-Mev excitation at $\theta_{lab} = 11^\circ, 17^\circ,$ and 25° , respectively. The states at 3.164 and 3.948 Mev

TABLE VI. $O^{18}(d,p)O^{19}$ measured absolute differential cross sections.

O^{19} energy level (Mev)	$\theta_{lab} = 11^\circ$ $d\sigma/d\Omega^a$ (mb/sr)	$\theta_{lab} = 17^\circ$ $d\sigma/d\Omega^a$ (mb/sr)	$\theta_{lab} = 25^\circ$ $d\sigma/d\Omega^a$ (mb/sr)
0 ± 0.030	16.0 ± 0.2	13.4 ± 0.6	8.54 ± 0.52
0.096	<0.36	<0.24	<0.13
1.469 ^b ± 0.011	21.7 ± 1.4	6.24 ± 0.83	3.56 ± 0.80
3.164 ± 0.030	1.35 ± 0.14	1.51 ± 0.16	0.59 ± 0.14
3.948 ± 0.030	3.23 ± 0.21	1.81 ± 0.20	0.86 ± 0.30
(4.123) ± 0.040	0.84 ± 0.15	0.40 ± 0.08	0.33 ± 0.07
(4.586) ± 0.040	0.54 ± 0.12	0.78 ± 0.09	0.58 ± 0.08
(4.706) ± 0.040	0.21 ± 0.15	0.34 ± 0.11	0.35 ± 0.08
(5.165) ± 0.040	1.43 ± 0.50	0.65 ± 0.20	0.38 ± 0.08
5.45 ^c	22.0 ± 3.3	17.6 ± 2.5	6.04 ± 0.91
5.707 ± 0.035	2.70 ± 0.24	2.28 ± 0.22	1.31 ± 0.16
6.279 ± 0.030	6.12 ± 0.63	4.82 ± 0.34	2.74 ± 0.29

^a Cross-section errors quoted in this table are relative, absolute cross sections having been determined by assuming the $O^{18}(d,p)O^{17}$ g.s. reaction ($E_d = 15$ Mev) cross section is 34 mb/sr at the peak of its angular distribution ($\theta_{cm} \approx 13^\circ$). See reference 13. All absolute cross sections quoted have an additional error of $\pm 25\%$. The 0.096-Mev state was not observed. Cross sections quoted for this level are statistical upper limits.

^b This value was taken from reference 20 and used as a standard. All other errors in excitation energies are estimated probable errors.

^c The broad peak (width ≈ 200 kev) corresponding to 5.45-Mev excitation in O^{19} consists of contributions from at least two unresolved levels.

³⁶ A. G. Blair and E. W. Hamburger (private communication).

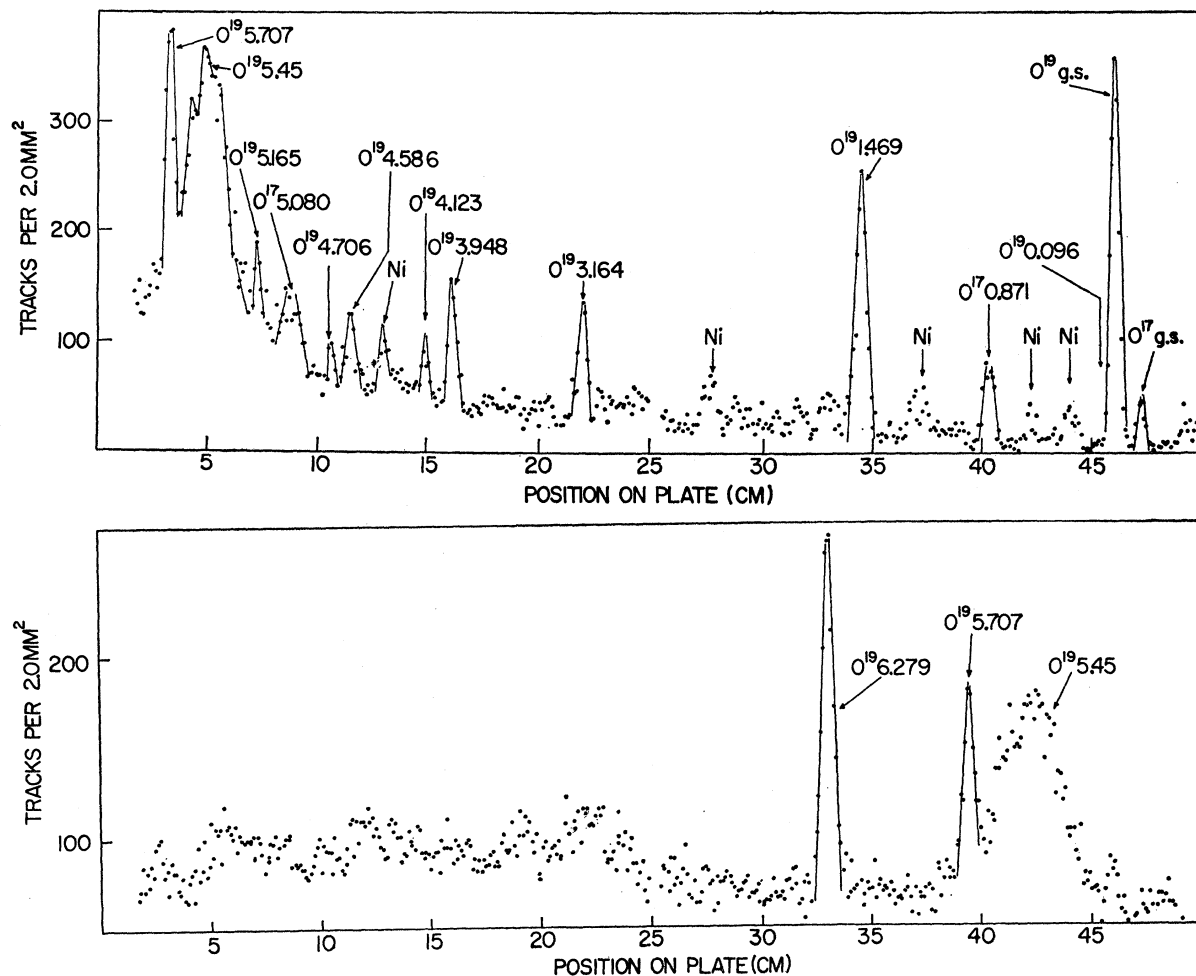


Fig. 12. Nuclear emulsion plate spectrum of $O^{18}(d,p)O^{19}$ reaction protons. Top figure shows 0- to 6-Mev excitation, bottom figure shows 5- to 9-Mev excitation, both at $\theta_{lab}=17^\circ$. Arrows denote the position of identified energy levels.

apparently correspond to those reported by Williams and Hough at 3.14 and 3.94 Mev.³⁷

Angular distributions of the well separated, positively identified O^{19} groups are shown in Fig. 13 through 18 together with curves calculated using the Butler-Born approximation. The only positively identified l_n values are those of the ground state ($l_n=2$) and the 1.469-Mev state ($l_n=0$) reactions. The $O^{18}(d,p)O^{19}$ 1.469-Mev reaction data were fitted with several $l_n=0$ curves, each having a different stripping radius. Experimental data for all other O^{19} states have been fitted with several curves having different l_n values by allowing large, and perhaps unreasonable, variations in the value of r_0 .

2. Analysis

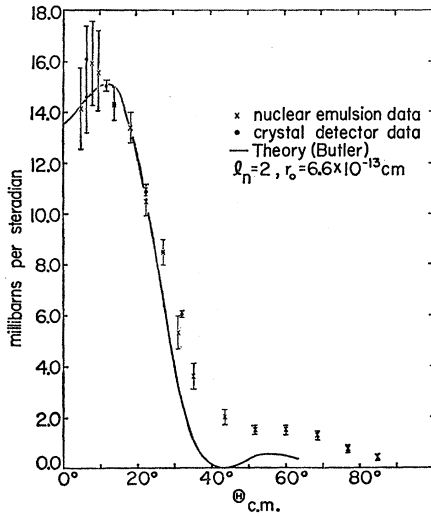
a. Spin, Parity, and Reduced-Width Values. The theoretical curves and experimental data presented in Figs. 13 through 18 have been used to extract the

quantity $[2J+1]\Theta^2$,¹⁷ and results are shown in Table VII.

TABLE VII. Parameters used in fitting theoretical curves to the $O^{18}(d,p)O^{19}$ angular distribution data.

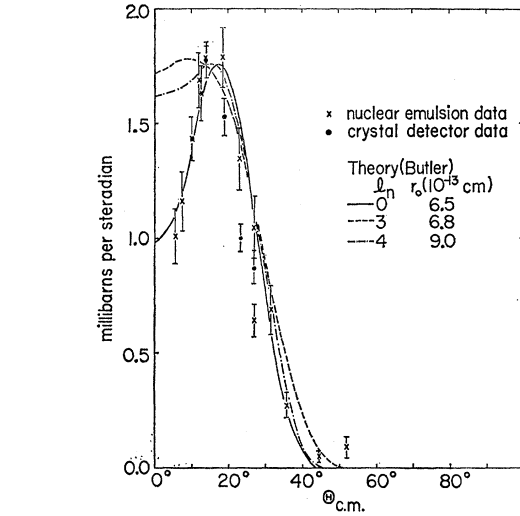
Level (Mev)	l_n	r_0 (f)	$[2J+1]\Theta^2$
g.s.	2	6.6	0.11
1.469	0	4.45	0.18
	0	4.8	0.32
	0	5.0	0.45
3.164	0	6.5	0.019
	3	6.8	0.016
	4	9.0	0.024
3.948	0	7.2	0.019
	1	4.6	0.012
	2	6.4	0.015
5.707	3	8.6	0.020
	0	4.7	0.012
	2	4.0	0.011
6.279	3	5.6	0.017
	0	5.0	0.022
	2	4.5	0.022
	3	6.0	0.033

³⁷ W. Williams, Jr., and P. V. C. Hough, Bull. Am. Phys. Soc. 4, 219 (1959).

FIG. 13. Angular distribution of the $O^{18}(d,p)O^{19}$ ground state.

The ground-state spin of O^{19} is known to be either $3/2$ or $5/2$. The theoretical $l_n=2$ curve fitted to the data of this group (Fig. 13) confirms this assignment and indicates positive parity. Table VII yields $\Theta^2=0.28$ if $J^\pi=3/2^+$ and $\Theta^2=0.18$ if $J^\pi=5/2^+$. Assuming $\Theta_0^2(1d)=0.05$,¹⁶ the spectroscopic factors are 0.56 and 0.36, respectively.

The possible spin and parity assignments for the 0.096-Mev state are $3/2^+$ and $5/2^+$. Assuming that this state has positive parity, its excitation via the $O^{18}(d,p)-O^{19}$ reaction would require the absorption of an $l_n=2$ neutron. The angular distribution of the proton group corresponding to the reaction would therefore be similar to that of the ground-state group and the ratio of $[2J+1]\Theta^2$ values for these reactions would be approximately equal to the ratio of their cross sections. This is because the Q values involved (1.6 and 1.7 Mev)

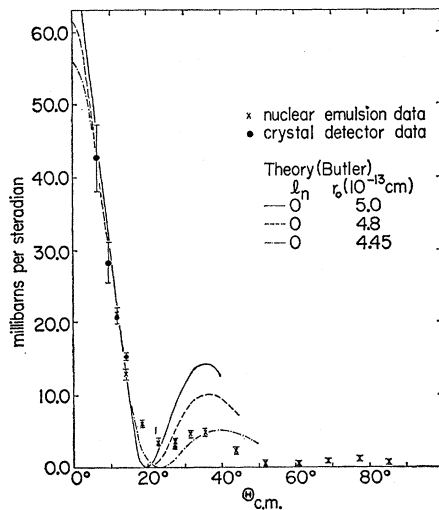
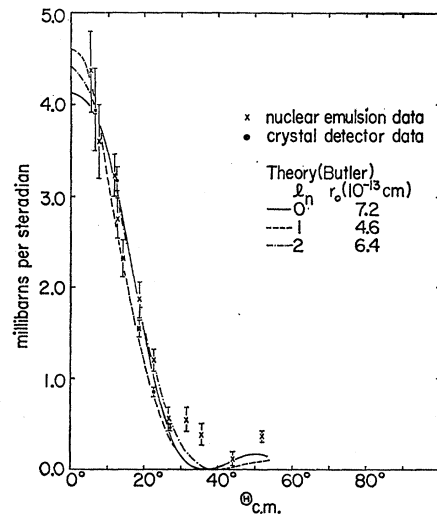
FIG. 15. Angular distribution of the $O^{18}(d,p)O^{19}$ 3.164-Mev state.

are nearly the same and the theoretical angular distribution is comparatively insensitive to small changes in Q value here. Thus the cross sections of Table VI indicate

$$\frac{[2J_0+1]\Theta^2(\text{ground state})}{[2J+1]\Theta^2(0.096\text{-Mev state})} \approx \frac{s(\text{ground state})}{s(0.096\text{-Mev state})} \geq 50$$

if the 0.096-Mev state has positive parity. This inequality together with theoretical calculations may be used to make tentative spin assignments for the relevant states.

Complete wave functions for the three lowest predicted states in O^{19} have been published by Redlich³ and by Elliott and Flowers.⁴ While inspection reveals differences in the wave functions of these two calculations, they are in essential agreement. For the low-

FIG. 14. Angular distribution of the $O^{18}(d,p)O^{19}$ 1.469-Mev state.FIG. 16. Angular distribution of the $O^{18}(d,p)O^{19}$ 3.948-Mev state.

lying $J^\pi=5/2^+$, $1/2^+$, and $3/2^+$ states the dominant configurations are $(d_{5/2}^3)_{5/2}$, $(d_{5/2}^2s_{1/2})_{1/2}$, and a combination of $(d_{5/2}^3)_{3/2}$ and $(d_{5/2}^2s_{1/2})_{3/2}$, respectively. We have seen that the O¹⁸ ground-state wave function is predominantly $(d_{5/2}^2)_0$ and it is apparent that the $l_n=2$ transition to the lowest $3/2^+$ in O¹⁹ can only proceed weakly.³⁸

Using the O¹⁸ ground-state wave function experimentally determined from the O¹⁸(d,t)O¹⁷ analysis and the theoretically predicted O¹⁹ wave functions of Redlich,³ the spectroscopic factors for the O¹⁸(d,p)O¹⁹ reactions to the low-lying $5/2^+$, $1/2^+$, and $3/2^+$ states in O¹⁹ have been calculated to be 0.62, 0.77, and 0.0004, respectively.

Both Redlich and Elliott and Flowers predict an O¹⁹ level order of $5/2^+$, $1/2^+$, $3/2^+$ extending over not more than 2 Mev. But, if all the levels in O¹⁹ below 3 Mev have been observed and if the predicted $5/2^+$ and $3/2^+$ states are among them, the experimental data are compatible only with the assignments

$$J^\pi(\text{O}^{19} \text{ ground state})=5/2^+,$$

and

$$J^\pi(\text{O}^{19} \text{ 0.096-Mev state})=3/2^+,$$

giving a $5/2^+$, $3/2^+$, and $1/2^+$ level order. These assignments are not at variance with any experimental data and if the assumptions made are valid, the evidence is conclusive. In particular, the theoretical ratio

$$S(J^\pi=3/2^+)/S(J^\pi=5/2^+) \approx 0.001$$

is so small that enormous inaccuracies in the theoretical O¹⁹ wave functions would be required to reverse the above assignments.

The O¹⁸(d,p)O¹⁹ 1.469-Mev state reaction data can be fitted only with $l_n=0$ curves and it may be concluded that

$$J^\pi(\text{O}^{19} \text{ 1.469-Mev state})=1/2^+.$$

The reduced width extracted for this transition is highly sensitive to the choice of the stripping radius. Using both the slope of the experimental data for $\theta_{c.m.} < 20^\circ$ and the position of the second maximum, the angular distribution of this group (Fig. 14) has been fitted with three values of r_0 . The agreement between the theoretical curves and the experimental data appears to be equally good for all three r_0 values, while the extracted reduced widths (Table VII) differ greatly. Although the normalized theoretical curves for $r_0=4.45f$ and $r_0=4.8f$ differ by only 10% at $\theta_{c.m.}=0^\circ$, the reduced widths resulting from these curves are in a ratio of approximately 1.8. Accurate quantitative analysis is obviously impossible, but for use in the discussion to follow it may be noted that, assuming $\Theta_0^2(2s)=0.16$,¹⁶ the spectroscopic factors for this transition are 1.3, 1.0, or 0.56 for r_0 values of 5.0f, 4.8f, and 4.45f, respectively.

Low-angle data for the 3.164-Mev state reaction

³⁸ This has been previously noted. W. Zimmermann, Phys. Rev. 114, 837 (1959).

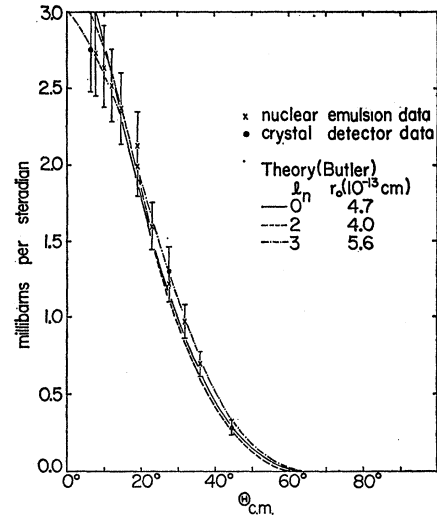


FIG. 17. Angular distribution of the O¹⁸(d,p)O¹⁹ 5.707-Mev state.

(Fig. 15) are best fitted by the $l_n=0$ curve, indicating $J^\pi=1/2^+$ for this state. The existence of two low-lying $1/2^+$ states separated by less than 2 Mev seems somewhat improbable, and in view of the fact that low-angle stripping data commonly disagree with theory it is concluded that this J^π assignment is questionable and will not be adopted here.

If the 5.45-Mev excitation group (Table VI), for which no angular distribution was obtained, contains a major contribution from a single state in O¹⁹, this transition would possess a relatively large reduced width. This group could not be resolved into its components, but its width (approximately 200 kev) does not preclude the possibility that it is primarily attributable to a single level. If this is the case, it is suggested that the large reduced width (i.e., large cross section) for this transition results from the fact that

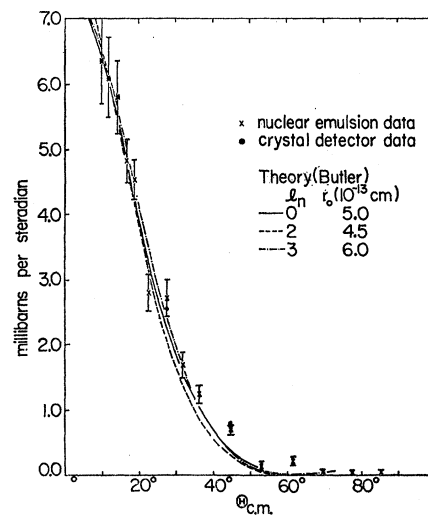


FIG. 18. Angular distribution of the O¹⁸(d,p)O¹⁹ 6.279-Mev state.

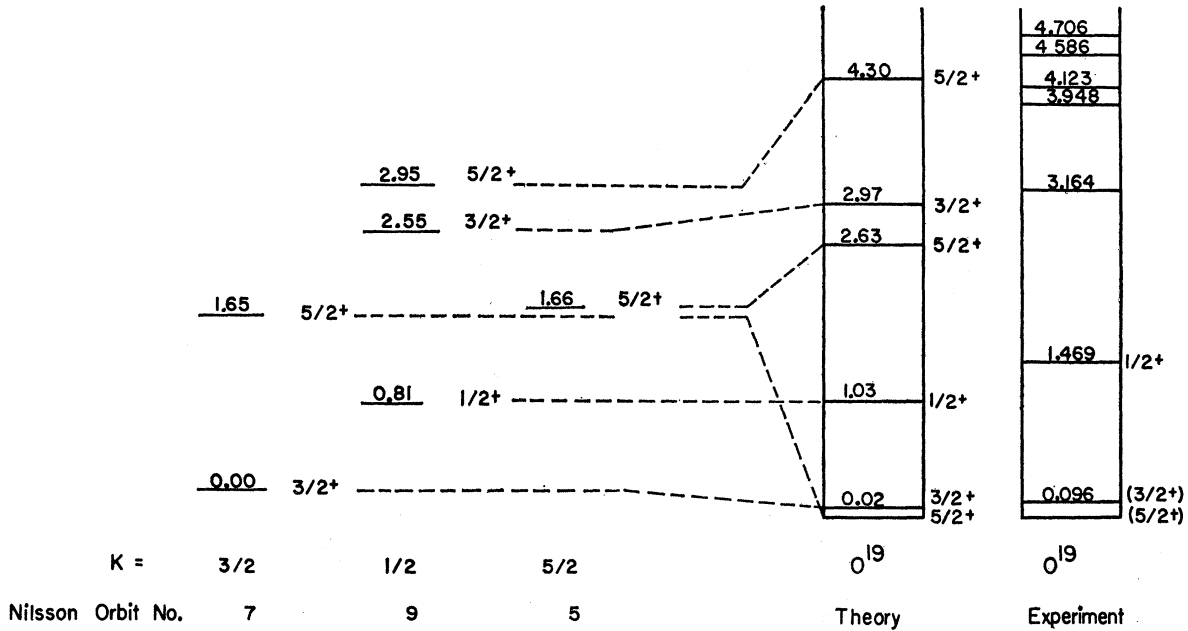


FIG. 19. Strong-coupling unified-model description of the low-lying states of O^{19} . The $J^\pi = \frac{1}{2}^+$, $\frac{3}{2}^+$, and $\frac{5}{2}^+$ states arising from Nilsson, reference (27), orbits 7, 9, and 5 are shown at the left (energies measured relative to the $\frac{3}{2}^+$ state of orbit 7). The final theoretical spectrum and experimental level diagram (up to 5-Mev excitation) are shown at the right. Parameter values used to obtain the theoretical spectrum are listed in Table VIII.

this state is to a large extent $(d_{5/2}^2 d_{3/2})_{3/2}$, although numerous other configurations are, without doubt, present in the function.

No angular distributions were obtained for the possible O^{19} states at 4.123, 4.586, 4.706, and 5.165 Mev and the similarity of various l_n curves fitted to the angular distribution of the 3.948-, 5.707-, and 6.279-Mev states prevents unique l_n determinations for them. The J^π assignments for all these levels therefore remain undetermined.

b. Strong-Coupling Unified Model Description of O^{19} . In applying the strong-coupling unified model to O^{19} the total Hamiltonian was taken to be of the form

$$H = \frac{\hbar^2}{2\mathcal{I}} [I^2 + J^2 - I_z^2 - J_z^2 - (I_+ J_- + I_- J_+)] + H_{\text{int}}, \quad (9)$$

where \mathcal{I} = moment of inertia of the nucleus, I = total angular momentum, J = particle angular momentum, z = nuclear symmetry axis, and H_{int} = intrinsic (i.e., individual particle) Hamiltonian. A description of the intrinsic motion commonly used in unified model calculations has been discussed by Nilsson and is used here.²⁷ The Hamiltonian consists of a deformed harmonic oscillator term, H_0 , to which is added spin-orbit and l^2 corrections:

$$H_{\text{int}} = H_0 + C \mathbf{I} \cdot \mathbf{s} + D l^2. \quad (10)$$

An extension of Nilsson's calculations for the $N=2$

$(1d-2s)$ shell has been made by allowing variations in $\mu = 2D/C$ from -0.2 to $+0.5$.³⁹

In order to apply this model to O^{19} it is necessary to know the values of various parameters which arise from the use of Eq. (9) and (10). These have been estimated by a variety of means and are summarized in Table VIII. The moment of inertia parameter $\hbar^2/2\mathcal{I}$ is taken from the position of the first excited state in O^{18} while the deformation has been estimated by assuming the validity of Rakavy's⁷ calculated ratio $\beta(O^{19})/\beta(F^{19}) \approx 3/4$ and taking $\beta(F^{19}) = 0.3$ as used

TABLE VIII. Parameters used with the strong-coupling unified model in describing O^{19} .

Parameter	Value	Reference
$l \cdot s$ splitting strength (C)	2.18 Mev	a
l^2 strength (D)	0.12 Mev	a
Moment of inertia parameter ($\hbar^2/2\mathcal{I}$)	0.33 Mev	b
Harmonic oscillator level spacing ($\hbar\omega_0^0$)	15.4 Mev	c
Nuclear deformation (β)	0.225	d
Nuclear deformation (δ)	0.214	e
Nilsson parameter (η)	3.0	e
Nilsson parameter (μ)	-0.1	e
Nilsson parameter (κ)	0.07	e

^a Calculated using the O^{19} energy level values; see text.
^b Calculated using the O^{19} energy level values taken from reference 20.
^c $\hbar\omega_0^0 = 41/A^{1/2}$; see reference 27.
^d β for O^{19} taken as $\frac{3}{4}\beta$ for F^{19} ; see reference 6 and 7.
^e Calculated using above parameters; see reference 27.

³⁹ These calculations were performed in collaboration with A. G. Blair and S. Meshkov.

previously by Paul.⁶ The values of C and D in Eq. (10) are taken from the O¹⁹ energy level spectrum by assuming the ground, 1.469-Mev, and 5.45-Mev states correspond to single-particle $1d_{5/2}$, $2s_{1/2}$, and $1d_{3/2}$ states, respectively.

The energy level spectrum of the low-lying states in O¹⁹ which results from using the complete unified Hamiltonian in the strong-coupling limit [Eq. (9)], the intrinsic Nilsson Hamiltonian [Eq. (10)], and parameters taken from Table VIII appears in Fig. 19. In Fig. 19 the unperturbed level order is shown at the left where each state is labeled by I . The value of K , the projection of I on the nuclear symmetry axis, appears under each rotational band together with Nilsson's designation (orbit number).

States with the same total angular momentum having K values differing by 1 (or both equal to $\frac{1}{2}$) interact through a coupling of the total angular momentum with the individual particle angular momentum (referred to as rotation-particle coupling or RPC). This interaction between unperturbed states yields the final level diagram labeled Theory in Fig. 19. The experimental energy level diagram is shown for comparison. The spin and parity order is in agreement with the J^π values deduced above and the theoretical energy values are in reasonable agreement with experiment, a ground-state spin of $5/2^+$ resulting theoretically from strong RPC interaction.

In addition the theoretical O¹⁸(d,p)O¹⁹ spectroscopic factors were calculated. The results for the low-lying $5/2^+$, $3/2^+$, and $1/2^+$ states are shown in Table IX together with those obtained from shell model wave functions and those observed experimentally. In view of the uncertainties in both the experimental data and the parameter values of Table VIII, the agreement between experiment and theory is most satisfactory. It is noteworthy that the S values obtained from the Nilsson calculation also agree with shell-model predictions.

Spectroscopic factors for the three states predicted above 2 Mev (Fig. 19) were also calculated. The S values are 0.0003, 0.15, and 0.005 for the ($5/2^+$) 2.63-, ($3/2^+$) 2.97-, and ($5/2^+$) 4.30-Mev states, respectively. If a $5/2^+$ state does exist at approximately 2.6 Mev, the small S would account for its nonobservance in the present experiment. The next $5/2^+$ state, predicted to lie at about 4.3-Mev excitation, could be any of the states observed between 4 and 5 Mev. It is unlikely that the $3/2^+$ state predicted to lie at 2.97 Mev corresponds to the experimentally observed state at 3.164 Mev. If the 3.164-Mev state possessed a spin of $3/2^+$, its angular distribution would be characterized by an $l_n=2$ stripping curve, but in order to fit the position of the observed maximum (Fig. 15) a theoretical $l_n=2$

TABLE IX. Spectroscopic factors for O¹⁸(d,p)O¹⁹ transitions to low-lying states.

J^π	Experiment ^a	Shell model	Nilsson
$5/2^+$	0.36	0.62	0.74
$3/2^+$	<0.007	0.0004	0.0008
$1/2^+$	0.56 to 1.3	0.77	0.46

^a The experimental S values are based on the J^π assignments deduced in the text and assuming $\Theta_{0^2}(1d)=0.05$ and $\Theta_{0^2}(2s)=0.16$.

curve requires a stripping radius less than $3f$ or greater than $9f$. It is more probable that this state has either negative parity or arises from intrinsic states lying higher than those considered in Fig. 19. The predicted $3/2^+$ state may correspond to the experimentally observed 3.948-Mev state. The experimental spectroscopic factor, 0.08, is in reasonable agreement with the theoretical value, 0.15.

The above theoretical description of O¹⁹ seems to explain adequately the experimentally observed low-lying level structure and reaction data. The calculation was based on parameter values obtained both from neighboring nuclei and from what are believed to be reasonable estimates. No arbitrary adjustment of any parameter was made and, in particular, the positions of the unperturbed states were calculated explicitly.

The theoretical results may be improved by altering one or more of the parameter values. Better agreement with the experimental level spectrum may be obtained by using a larger value of C , a smaller value of D , or a larger moment of inertia parameter. Similarly, the theoretical spectroscopic factors can be adjusted to give better agreement with experiment by choosing a smaller deformation parameter. In view of the lack of spin and parity assignments for states above 3-Mev excitation, it is felt that any attempt at this time to improve the theoretical results by arbitrary adjustment of these parameter values would be meaningless. A true estimate of the model's success can be made only after comparison with further experiments, in particular, those dealing with the dynamic properties of this nucleus.

ACKNOWLEDGMENTS

One of us (J. C. A.) is grateful to the National Science Foundation for the grant of fellowships during the course of this research. Appreciation is expressed to Dr. N. Austern, Dr. E. U. Baranger, Dr. M. H. Macfarlane, and Dr. S. Meshkov for helpful discussions and criticisms. The assistance and active interest throughout all phases of this work by A. G. Blair and E. L. Keller is gratefully acknowledged as is the support and encouragement of Dr. A. J. Allen.